*URSI-RCRS 2024, ARIES/GEHU, Bhimtal, India, 22 - 25 October, 2024*

# The prediction of rapid response of Equatorial electrojet (EEJ) to Interplanetary (IP) shocks

B. Nilam, and S. Tulasi Ram
Indian Institute of Geomagnetism, Mumbai, India

## Abstract

Interplanetary (IP) shocks are one of the dominant solar wind structures that can significantly affect the Geospace when impinge on the magnetosphere. A series of magnetospheric-ionospheric disturbances are triggered, e.g., steepening of non-linear magnetosonic waves, enhanced Chapman-Ferraro currents, Field-Aligned Currents, high-latitude convection, auroral currents, and prompt penetration electric fields, etc. The Equatorial Electrojet (EEJ), a proxy for the equatorial ionospheric electric field, also changes rapidly upon the impact of IP shocks. Abrupt geomagnetic field disturbances during IP shocks can exceed 100 nT/min at equatorial latitudes due to the changes in EEJ, potentially causing Geomagnetically Induced Currents (GICs). Additionally, the increase in the equatorial electric field during IP shocks can enhance E×B plasma drift, leading to the intensification of the Equatorial Ionization Anomaly (EIA). Furthermore, an increase in the electric field following an IP shock during post-sunset hours can lead to the occurrence of equatorial plasma bubbles, and significant electron density depletions, which substantially disrupt the radio communications. Hence, monitoring changes in the EEJ during IP shock arrivals is crucial for understanding space weather, emphasizing the necessity of predicting EEJ changes in such events. In this study, 306 IP shock events occurring between 2001, and 2022 were analyzed to investigate the response of EEJ to these disturbances. Finally, an empirical model was developed to quantitatively estimate the EEJ response to IP shocks over Indian sector. This model incorporates key parameters, including variations in solar wind dynamic pressure, shock impact angle, interplanetary electric field, solar flux (F10.7), and local time. Despite the coefficients of the empirical model being optimized for the Indian sector, they still provide reliably accurate estimations of EEJ in other longitudinal sectors. The EEJ response to an IP shock during a superstorm occurred on 10 May 2024 was calculated using this empirical relation for two different locations, Tirunelveli (UT+5), and Huancayo (UT-5). The observed EEJ responses ($\Delta EEJ_{TIR}$ = -17nT, $\Delta EEJ_{HUA}$= 121nT) closely matched with the estimated values ($\Delta EEJ_{TIR}$ = -18nT, $\Delta EEJ_{HUA}$= 136nT), demonstrating the effectiveness of this empirical model in predicting such responses. This predictive capability is crucial for understanding variations in the equatorial ionosphere, thereby aiding the mitigation of space weather effects in advance.

## 1. Introduction

When a fast flow of solar wind disturbances associated with Coronal Mass Ejections (CMEs) or Corotating Interaction Regions (CIRs), travels through interplanetary space, it can create a shock front if it moves faster than the magneto-sonic speed of the medium. These shock fronts are known as "Interplanetary (IP) shocks" which causes sudden and noticeable increases in the speed, temperature, density, and magnetic field of the solar wind, due to the waves being squeezed together and creating a pressure jump. The sudden enhancement of solar wind dynamic pressure ($P_{Dyn}$) associated with IP shocks could induce convection electric fields at high-latitude ionosphere which can promptly penetrate to equatorial and low-latitude regions. Additionally, prompt penetration electric field disturbances may also be induced due to the sudden southward/northward turnings of the Interplanetary Magnetic Field (IMF Bz) (eastward/westward turnings of the interplanetary electric field, IEFy) during IP shocks. The resultant electric field disturbances can significantly alter the ionospheric electrodynamics and equatorial electrojet (EEJ).

Penetration of high-latitude convection electric fields and the associated geomagnetic field disturbances can have significant consequences in the equatorial ionosphere. The enhanced dawn-to-dusk electric fields at the equatorial latitudes drive strong Equatorial Electrojet (EEJ) current (Kikuchi et al., 2001; Tulasi Ram et al., 2008), enhanced vertical ExB plasma drifts (Tulasi Ram et al., 2016) and the rejuvenation of Equatorial Ionization Anomaly (EIA) (Tulasi Ram et al., 2019) during daytime. The rapid geomagnetic field disturbances during IP shocks can often be as large as 100 nT/min at equatorial latitudes due to the presence of the EEJ and can cause Geomagnetically Induced Currents (GIC) (Nilam & Tulasi Ram, 2022; Oliveira et al., 2018). Therefore, monitoring changes in the EEJ during IP shock arrival is crucial for understanding space weather, highlighting the need of predicting EEJ changes in these events. Accurate predictions can help mitigate the adverse effects on communication, and navigation systems.

The EEJ response to numerous IP shocks from 2001 to 2022 has been examined in the present study. The magnitude of the EEJ response to IP shocks shows a clear local time dependence, and varies linearly with the change in $P_{Dyn}$. The EEJ response is also found to depend considerably on the solar activity (F10.7 solar flux), shock impact angle, and IEFy associated with IP shocks. For the first time, an empirical relation is derived that can predict the rapid EEJ response to IP shocks. The derived empirical relation is found to be very accurate in predicting the response of the EEJ, and exhibits an excellent correlation with observations. Since the empirical model is based on solar wind parameters measured at the Lagrangian L1 point, it provides a lead time of 40-60 minutes. Therefore, this model is also valuable for real-time prediction of the response of EEJ to IP shocks.

## 2. Data

The fast forward IP shocks during the period 2001 – 2021 were selected from the published IP shock database by Oliveira, [2023] (available at https://zenodo.org/records/7991430). The corresponding solar wind density, velocity, IMF, and IEFy data were taken from ACE, and Wind satellite observations. A pair of equatorial-low latitude ground-based magnetometers at Tirunelveli (TIR, 8.7°N, 77.8°E, 1.5°N dip latitude), and Alibag (ABG, 18.6°N, 72.9°E, 11.99°N dip latitude) from the Indian longitude sector are considered to study the EEJ variations during these IP shocks. The difference of ΔH values between equatorial, and off-equatorial, represents the EEJ strength [Rastogi, 1977]. Another pair of equatorial-low latitude ground-based magnetometers at Hauncayo (HUA, 5.17°S, 80.65°W, , 1.17°N dip latitude), and Piura (PIU, 12.06°S, 72.9°E, 7.3°N dip latitude) are used to validate the prediction of the empirical model for an IP shock arrived on 10 May 2024.

## 3. Results and Discussion

Interplanetary shocks are marked by abrupt increases in solar wind velocity, density, temperature, and magnetic field strength. We have considered a total of 306 IP shocks during the period 2001-2021 which are further separated into day (0600-1800 LT), and night (1800-0600 LT) time events considering the local time. Figure 1 represents the superposed epoch analysis for changes in the total IMF, $P_{Dyn}$ (indicates change in velocity, and density), and the dawn-dusk component of the IEF for the 162 day-time (left panels), and 144 night-time (right panels) IP shock events. The light green curves indicate the individual events whereas the thick black curve represents the mean variation. The X-axis indicates the epoch time in minutes, and the vertical line corresponds to the time of shock onset. All the parameters are shifted to zero at the onset time of shock by subtracting the values corresponding to the zero epoch time. The bottom panel shows the response of EEJ to IP shock during day, and night-time. Since the magnetopause current is not expected to exhibit significant difference between the two stations that are separated by ~10 latitude, the observed difference can be mainly attributed to enhancements in EEJ.

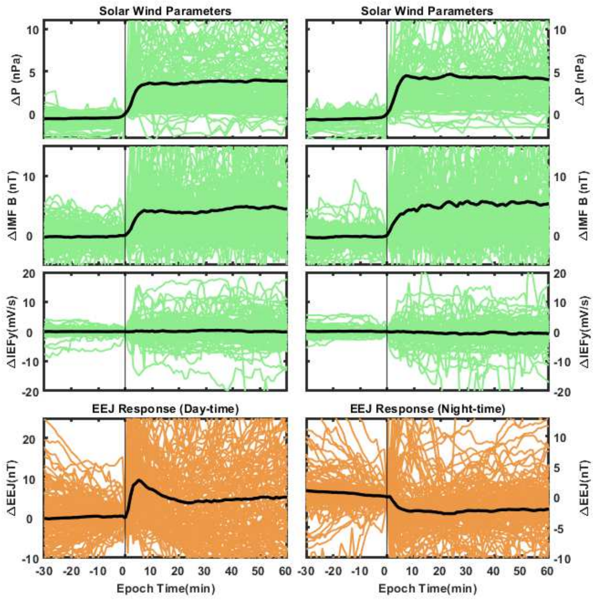


**Figure 1.** The left, and right hand side panels show the variations of solar wind parameters for day-time, and night-time response of EEJ during IP shock events.

In order to examine the different influencing factor during arrival of IP shocks, the magnitudes of EEJ change (ΔEEJ) for the 306 events are plotted as a function of local time in Figure 2a. The blue dots represent the change in ΔEEJ while the red curve with error bar indicates the mean variation. It can be seen from this figure that the ΔEEJ exhibits significant local time variation, and reaches a maximum around pre-noon hours, and mostly negative during the night-time, and the magnitudes are much smaller. The smaller values during night-time are mainly due to low ionospheric conductivity. This suggests the major dependence of local time on the EEJ response to IP shock.

Even though the ΔEEJ is majorly dependent on local time, the large error bars in Figure 2a indicate a significant scatter in ΔEEJ due to other contributing factors. Thus, in order to further examine the role of $P_{Dyn}$ on the change in EEJ during the IP shocks, the ΔEEJ values are plotted against the $\Delta\sqrt{P_{Dyn}}$ as shown in Figure 2b. The red, and blue dots represent the IP shock events that occurred during the day and night times, respectively. The straight lines in red and blue colors represent the corresponding linear regression fits. As can be noticed, the ΔEEJ exhibits linear positive and negative correlations with $\Delta\sqrt{P_{Dyn}}$ during day, and night times, respectively, and the corresponding correlation coefficients are indicated in the figure. Therefore, sudden enhancement in $P_{Dyn}$ during the IP shocks drives prompt penetration of eastward, and westward disturbances in the ionospheric zonal electric field during day, and night times, respectively. Though the ΔEEJ exhibits linear correlation with $\Delta\sqrt{P_{Dyn}}$, the large scatter in data points leads to a smaller correlation coefficient, particularly during day-time. This suggests that although $\Delta\sqrt{P_{Dyn}}$ causes significant changes in EEJ, the magnitude of EEJ response (ΔEEJ) does not depend solely on $\Delta\sqrt{P_{Dyn}}$.

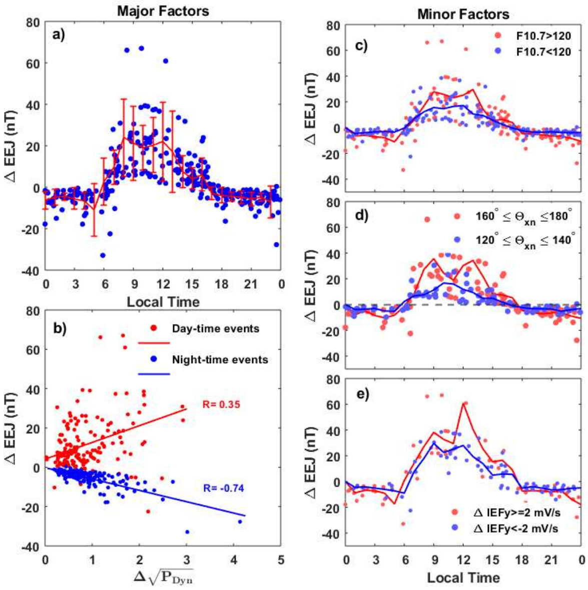


**Figure 2.** a) Local time variation of ΔEEJ in response to IP shocks, (b) variation of ΔEEJ with respect to $\Delta\sqrt{P_{Dyn}}$ during the day (red) and night (blue) times, variation of ΔEEJ for larger value (red) and smaller value (blue) of (c) solar flux (F10.7), (d) Shock Impact angle ($\theta_{xn}$), and (e) IEFy

Other minor factors that could contribute to the magnitude of the EEJ response to IP shocks are investigated. The ionospheric conductivity in the E region is expected to vary significantly during high and low solar activity periods and thereby influences the EEJ response. Hence, we separated the IP shock events that occurred during high (F10.7 solar flux >=120 $10^{-22}Wm^{-2}Hz^{-1}$) and low (F10.7 solar flux<120 $10^{-22}Wm^{-2}Hz^{-1}$) solar activity periods. Figure 2c shows the ΔEEJ variations during high (red dots) and low (blue dots) solar activity periods as a function of local time. The red and blue solid curves represent the 2-hour running mean variations of ΔEEJ during high and low solar activity periods, respectively. As one can notice, the ΔEEJ exhibits larger values during high solar activity (red curve) compared to low solar activity (blue curve) periods. The IP shock impact angle ($\theta_{xn}$) also plays a role in controlling the equatorial electrojet (EEJ) response. In order to bring out the differences in EEJ response, the shocks are classified into two groups i.e., nearly frontal shocks ($160^o \leq \theta_{xn} \leq 180^o$) and highly inclined shocks ($120^o \leq \theta_{xn} \leq 140^o$). According to this classification, 95 nearly frontal and 87 highly inclined IP shock events were found among the total of 306 IP shocks considered in this study. Figure 2d depicts the EEJ responses (ΔEEJ) for these two groups as a function of local time, with red, and blue circles representing nearly frontal, and highly inclined shocks, respectively. The red, and blue curves represent the two-hour running mean variations of ΔEEJ for the frontal and inclined shocks, respectively. Both curves exhibit similar local time variations, however, the magnitude of EEJ response is significantly stronger for the frontal shocks (red curve) during both day, and night times. This result emphasizes the role of shock impact angle on the EEJ response during all local times.

IP shocks are often associated with sudden changes in the east-west component of the Interplanetary Electric Field. The rapid variations in the IEFy are known to cause significant changes in the EEJ via prompt penetration electric field (PPEF) [Tulasi Ram et al. 2008]. Hence, the PPEF disturbances associated with the significant change in IEFy (say |ΔIEFy|≥ 2 mV/m) during IP shocks could positively or negatively augment the response of EEJ depending on the polarity of the change in IEFy. Figure 2e shows the local time variation of ΔEEJ during the IP shocks that are associated with increases (ΔIEFy > 2 mV/m), and decreases (ΔIEFy < -2 mV/m) in IEFy (red and blue dots, respectively). The red, and blue solid curves represent the respective 2-hour running mean variations. Clearly, one can observe that the increase in IEFy (positive ΔIEFy) during the IP shocks gives rise to higher ΔEEJ values compared to those events associated with the decrease in IEFy (negative ΔIEFy), particularly during day-time. This indicates that the eastward/westward PPEFs associated with positive/negative ΔIEFy augments/reduces the EEJ response during the IP shocks.

The results derived in Figures 2a to 2e suggest that the changes in $P_{Dyn}$, background solar flux levels, shock impact angle, and IEFy can contribute to the observed EEJ response during IP shocks IEFy at a particular local time. Hence, in order to account for the effects of interplanetary electric field changes, and background solar flux, the equation (1) is derived by considering these factors.

$$\Delta EEJ = \left(\left(0.1 + 0.1\, e^{\frac{\theta_{xn}-147}{37}}\right) \Delta\sqrt{P_{Dyn}} + 0.008\, \Delta IEF_y\right) \cdot F10.7 \cdot Real\left[cos^{1.47}\left(15\,(LT - 11.2)\right)\right] - 2.5 \qquad (1)$$

The coefficients of equation (1) were obtained by the non-linear least square fitting of observed ΔEEJ values for the 306 IP shocks considered in this study, and the comparison between observed, and predicted response of EEJ is shown in Figure 3. An excellent correlation can be observed between the estimated, and observed ΔEEJ values, with a correlation coefficient of 0.89, and Root Mean Square Error of 6.3 nT. The slope of the regression fit is also unity with nearly zero intercept. Therefore, equation (1) gives the best estimate of EEJ response during IP shocks by including the effects due to local time, $\Delta\sqrt{P_{Dyn}}$, $\theta_{xn}$, ΔIEFy, and F10.7 solar flux.

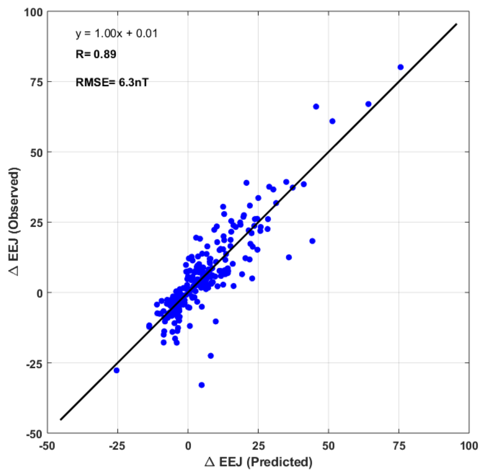


**Figure 3.** The predicted, and observed change in EEJ in response to IP shocks.

To validate the empirical model, an IP shock arrived on 10 May 2024 (1706UT) was considered, and it was not included in the previous statistical study. The empirical model delivers excellent results for the Tirunelveli location, with the observed ΔEEJ being -17nT, and the estimated ΔEEJ about -18nT. The solar wind parameters, and EEJ response for this IP shock is shown in Figure 4.

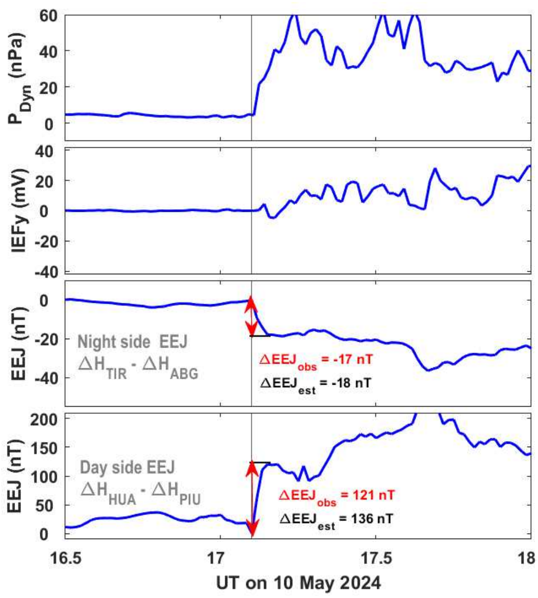


**Figure 4**. The predicted, and observed response of EEJ for IP shock arrived on 10 May 2024

In order to verify the dayside response of EEJ to the same shock, the EEJ at Haucayo location has been examined. Although the coefficients of equation (1) are optimized for Indian sector, they are still expected to yield reasonably accurate estimates of EEJ response at other longitude sectors as well. This is because, except for the longitudinal variation in ionospheric conductivity, the other influencing factors in equation 1 are global in nature. The coefficients in equation (1) can be used for other longitudinal sectors and verified the results with the observations available at the Hauncayo location. The equation (1) gives reliable estimation of the response of EEJ to IP shock. The estimated ΔEEJ at Haucayo is 136 nT, which closely matches the observed ΔEEJ value of 121 nT. Therefore, the empirical model is applicable for the prediction of EEJ response to IP shock at other longitude sector with minimal error.

## 4. Summary

In this study, a statistically significant number (306 cases) of IP shocks that occurred during 2001–2022 have been considered to investigate the response of EEJ from the Indian sector. The various factors that contribute to the prompt changes in EEJ during the IP shocks are investigated. It is found that the EEJ exhibits a major dependence on local time, and $P_{Dyn}$, and a relatively minor dependence on solar activity, $\theta_{xn}$, and IEFy. Eventually, an empirical model is developed which can quantitatively estimate the change in EEJ in response to IP shock by taking the above factors into account.

## 5. References


Kikuchi, T., Tsunomura, S., Hashimoto, K., & Nozaki, K. (2001). Field-aligned current effects on midlatitude geomagnetic sudden commencements. Journal of Geophysical Research, 106(A8), 15555–15565. https://doi.org/10.1029/2001ja900030

Nilam, B., & Tulasi Ram, S. (2022). Large geomagnetically induced currents at equator caused by an interplanetary magnetic cloud. *Space Weather*, 20(6), e2022SW003111 https://doi.org/10.1029/2022sw003111

Oliveira, D. M. (2023). Interplanetary shock data base. *Frontiers in Astronomy and Space Sciences*, 10, 1240323. https://doi.org/10.3389/fspas.2023.1240323

Oliveira, D. M., Arel, D., Raeder, J., Zesta, E., Ngwira, C. M., Carter, B. A., et al. (2018). Geomagnetically induced currents caused by interplanetary shocks with different impact angles and speeds. *Space Weather*, 16(6), 636–647. https://doi.org/10.1029/2018sw001880

Rastogi, R. G. (1977). Geomagnetic storms and electric fields in the equatorial ionosphere. *Nature*, 268(5619), 422–424. https://doi.org/10.1038/268422a0

Tulasi Ram, S., Nilam, B., Balan, N., Zhang, Q., Shiokawa, K., Chakrabarty, D., et al. (2019). Three different episodes of prompt equatorial electric field perturbations under steady southward IMF Bz during St. Patrick's Day storm. *Journal of Geophysical Research: Space Physics*, 124(12), 10428–10443. https://doi.org/10.1029/2019ja027069

Tulasi Ram, S., Yokoyama, T., Otsuka, Y., Shiokawa, K., Sripathi, S., Veenadhari, B., et al. (2016). Duskside enhancement of equatorial zonal electric field response to convection electric fields during the St. Patrick's Day storm on 17 March 2015. *Journal of Geophysical Research: Space Physics*, 121(1), 538–548.

Tulasi Ram, S., Rama Rao, P. V. S., Prasad, D. S. V. V. D., Niranjan, K., Gopi Krishna, S., Sridharan, R., & Ravindran, S. (2008). Local time dependent response of postsunset ESF during geomagnetic storms. *Journal of Geophysical Research*, 113(A7), A07310. https://doi.org/10.1029/2007JA012922